Time-Resolved EPR Study on Reorganization Energies for Charge Recombination Processes in Nanometer-Separated Radical Ion Pairs

Tomoaki Yago,[†] Yasuhiro Kobori,[†,‡] Kimio Akiyama,[†] and Shozo Tero-Kubota*[,†]

Institute of Multidisciplinary Research for Advanced Materials, Tohoku University, Sendai 980-8577, Japan, and PRESTO, Japan Science and Technology Corporation, Kawaguchi, Japan

Received: May 6, 2002; In Final Form: July 16, 2002

The reorganization energies for the intermolecular charge recombination processes have been determined for the electron donor−acceptor systems involving the quinones and methoxy aromatic molecules by time-resolved EPR and cyclic voltammetry measurements in polar solvents. We have carefully examined what distance between the donor and acceptor molecules is effective for the radical pair mechanism (RPM) chemically induced dynamic electron polarization (CIDEP) detection using the stochastic Liouville equation on the basis of the charge transfer (CT) interaction mechanism in the singlet−triplet energy splitting ($2J$) in radical ion pairs. The RPM CIDEP shows that the signs of the J are inverted from positive to negative with decreasing temperature. The results are interpreted by the CT interaction mechanism. With the observations of the $J \sim 0$ condition, the individual values of the total and solvent reorganization energies (λ_S) are determined for several 1.2 nm separated donor−acceptor systems. The individual λ_S values ranging from 1.27 to 1.39 eV in the present donor−acceptor systems agree with those calculated from the Marcus continuum dielectric model at 1.2 nm donor−acceptor separation within the deviation of ∼0.1 eV. In the dimethoxynaphthalene (DMN)−duroquinone (DQ) system, the solvent reorganization around the methoxy groups is dominated due to the localization of the electron spin density in the DMN cation radical.

Introduction

Photoinduced electron transfer (ET) reactions between neutral electron donor (D) and acceptor (A) molecules result in the formation of the geminate radical ion pairs (RIPs) in polar solvents.[1] The ET processes of the RIPs have been analyzed on the basis of the Marcus theory.[2,3] According to the classical Marcus theory, the rate constant (k_{CR}) of charge recombination (CR) in the RIP is represented as follows:[2b]

$$k_{CR}(r) = \sqrt{\frac{\pi}{\hbar^2 \lambda(r) k_B T}} V(r)^2 \exp\left[-\frac{\{\Delta G_{CR} + \lambda(r)\}^2}{4\lambda(r) k_B T}\right] \quad (1)$$

where $\lambda(r)$, $V(r)$, and $-\Delta G_{CR}$ are the reorganization energy, the electronic coupling matrix element, and the driving force for the CR reaction, respectively. The V and λ terms depend on the center-to-center separation of r between the D and A molecules in the solvent-separated RIP (SSRIP) systems. In the intermolecular ET reactions, Mataga et al. first observed the bell-shaped $-\Delta G_{CR}$ dependence of the k_{CR} for the SSRIP systems, demonstrating that the λ plays an important role to control the ET reaction rate as represented by eq 1 in the flexible RIP systems. [4]

The total reorganization energy of λ is partitioned into solvent reorganization energy (λ_S) and intramolecular vibrational reorganization energies (λ_V^D, λ_V^A) for the D and A molecules.[2,5]

$$\lambda(r) = \lambda_S(r) + \lambda_V^D + \lambda_V^A \quad (2)$$

The λ_S has been represented by the continuum dielectric model as follows:[3]

$$\lambda_S(r) = \frac{e^2}{4\pi\epsilon_0}\left(\frac{1}{2d_A} + \frac{1}{2d_D} - \frac{1}{r}\right)\left(\frac{1}{n_D^2} - \frac{1}{\epsilon}\right) \quad (3)$$

where d_D and d_A are radii of the D and A molecules, respectively. The permittivity constant of vacuum, refractive index and dielectric constant of solvents are represented by ϵ_0, n_D, and ϵ respectively. The λ_S values have normally been estimated by fitting the bell-shaped Marcus plot in the SSRIP systems at $r = 0.6 \sim 0.8$ nm.[4,6] In the Marcus plot, experiments are needed for many different reactant species to obtain a reorganization property. The obtained λ_S value does not reflect an individual reorganization property for one D−A system. Additionally, it has been quite difficult to specify the effective separation of r for the CR processes in the SSRIP systems that can undergo the diffusion motion.[7] When the relation of $-\Delta G_{CR} < \lambda$ is satisfied at the closest D−A distance of d, there exists a region of r ($> d$), where the optimum condition ($-\Delta G_{CR} = \lambda$) is satisfied for the CR process, because the λ_S increases with r as shown eq 3. As a result, the effective r for the CR varies for the D−A systems, depending on the λ and on the $-\Delta G_{CR}$ values. Moreover, several studies[8] suggested that the solute steric effects influence the effective r of the ET reactions in the SSRIP systems. Therefore, it is not clear whether the continuum dielectric model of eq 3 is really applicable for the individual flexibly separated D−A molecular systems because of the uncertainty of the ET distance of r for the liquid-phase bimolecular reactions.

The time-resolved electron paramagnetic resonance (TREPR) measurements of the chemically induced dynamic electron polarization (CIDEP) give us the information on the short-lived

* Corresponding author. Telephone +81-22-217-5612; fax +81-22-217-5612. E-mail tero@tagen.tohoku.ac.jp
† Tohoku University.
‡ PRESTO.

10.1021/jp021119s CCC: $22.00
Published on Web 09/10/2002

CHART 1

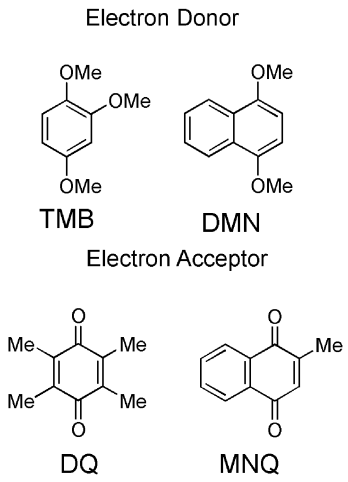

paramagnetic species including the RIPs.[9−14] The radical pair mechanism (RPM) CIDEP[10] is originated from the electron spin interactions in the solvent separated radical pair. Under the external magnetic field, the singlet−triplet mixing ($S-T_0$ mixing) is induced by the hyperfine coupling interaction (HFI) and by the effect of the Zeeman energy difference (Δg effect) in the solvent-separated radical pairs. The intermolecular interaction of the $2J$ is defined as the energy splitting between the singlet and triplet radical pairs. The operation of the J after the certain $S-T_0$ mixing induces the RPM CIDEP during the process of the diffusion in the radical pairs. The RPM CIDEP is effectively generated where the magnitude of the $2J$ is comparable to that of sum of the HFI and the Δg effect.[10] The polarization patterns of the RPM CIDEP spectra depend on the spin multiplicity of the reaction precursor states and the sign of the J.

Recent CIDEP studies[13,14] verified that the charge-transfer interaction (J_{CT}) dominates the J of RIPs. According to the J_{CT} mechanism, the J of RIP is induced by the electronic coupling perturbation from the charge-recombined states at the equilibrium solvent and solute configurations in the RIPs.[13−15] In our previous study, we briefly reported that the individual λ value for a 1.2 nm separated D−A system can be determined by the observation of the RPM CIDEP in the RIP of the 1,2,4-trimethoxybenzene (TMB) cation−duroquinone (DQ) anion radical system.[5]

In this paper, we have determined the individual λ values for the several solute molecular systems (Chart 1) to evaluated the applicability of the Marcus model in eq 3 for the D−A systems at $r = 1.2$ nm, by observing the temperature dependences of the RPM CIDEP in the RIPs.

Experimental Section

DQ (Tokyo Kasei, GR-grade), 2-methyl-1,4-naphthoquinone (MNQ; Nacalai tesque, GR-grade), and 1,4-dimethoxynaphthalene (DMN; Aldrich) were recrystallized from ethanol. TMB (Tokyo Kasei) was used as received. Butyronitrile (BuN; Tokyo Kasei, GR grade) and *N*,*N*-dimethylformamide (DMF; Nacalai tesque, GR grade) were used as the solvents.

The TREPR measurements were performed by using an X-band EPR spectrometer (Varian model E-109E) without field modulation. The transient EPR signals were transferred to a wide band amplifier and were taken into a boxcar integrator (EG & G Princeton Applied Research model 4162). A Nd:YAG laser (Quanta-Ray GCR-14S, 355 nm) was used for the excitation of the acceptor quinones. The sample solutions were deoxygenated by argon gas and flowed into a quartz flat cell (0.5 mm inner space) in the EPR cavity. A nitrogen flow cryostat was used to control the temperature. The concentrations of the solutes were 5.8×10^{-3}∼1.2×10^{-2} M for the quinones and 1.2×10^{-2}∼2.0×10^{-2} M for TMB and DMN.

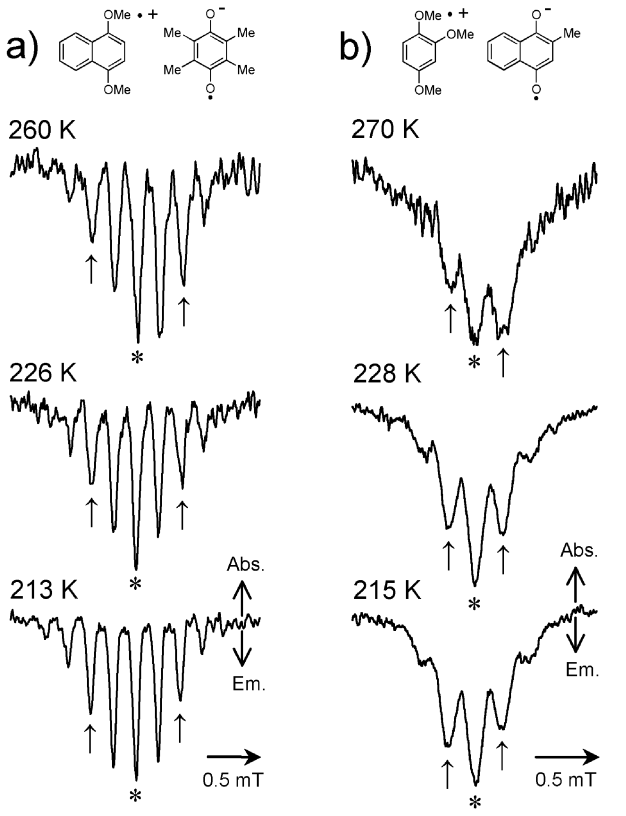

Figure 1. Temperature effects on the CIDEP spectra observed at 500 ns after the 355 nm laser pulse excitation of the systems of (a) 1,4-dimethoxynaphthalene (2.0×10^{-2} M)−duroquinone (2.0×10^{-2} M) and of (b) 1,2,4-trimethoxymbenzene (1.2×10^{-2} M)−2-methyl-1,4-naphthoquinone (5.8×10^{-3} M) in butyronitrile. The asterisks indicate the center of the hyperfine structure of the corresponding quinone anion radicals.

The cyclic voltammetry (CV) measurements were performed with the three-electrode system consisting of a voltammetric analyzer (Yanagimoto P-1000) with platinum working electrodes and a saturated calomel reference electrode (SCE). Solute concentrations were 3×10^{-3} M. Tetra-*n*-butylammonium perchlorate (TBAP; 0.06 M, Nacalai tesque, electrochemical grade) and tetra-*n*-propylammonium perchlorate (TPAP; 0.1 M, Nacalai tesque, electrochemical grade) were used as the supporting electrolytes in BuN and in DMF, respectively. Scan rates were 0.02∼0.5 V s^{-1}. A homemade cell was used to control the temperature. Details of the equipments for temperature control were reported in Supporting Information of ref 5.

Results

Temperature Dependences of the Sign of the J and $-\Delta G_{CR}$. Figure 1a shows the temperature effect on the CIDEP spectra observed at the delay time of 500 ns after the laser excitation of DQ (1.2×10^{-2} M) in the presence of DMN (2.0×10^{-2} M) in BuN. The signals were assigned to the DQ anion radical ($DQ^{\bullet -}$) from the g value and hyperfine coupling constants (HFCs) ($g = 2.0049$, $a^{H}_{Me} = 0.192$ mT).[16] In the original TREPR spectra, the broad emission signals due to the DMN cation radical ($DMN^{\bullet +}$: $g = 2.0032$, $a^{H}_{Me} = 0.219$ mT,

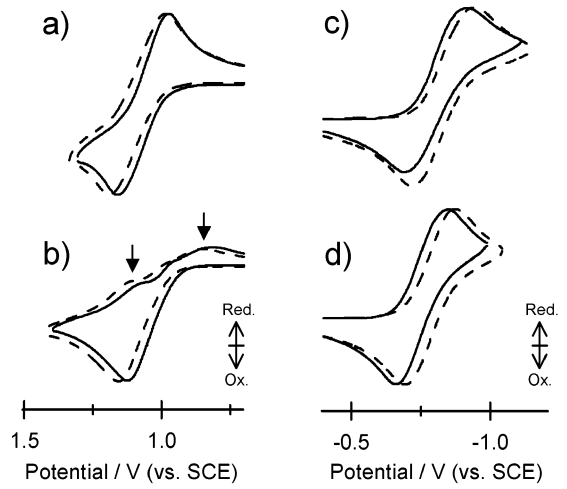

Figure 2. Cyclic voltammograms of (a) 1,4-dimethoxynaphthalene observed at 226 K with the scan rate of 0.05 V s^{-1}(—) and at 260 K with the scan rate of 0.1 V s^{-1}(- -), (b) 1,2,4-trimethoxybenzene; 228 K, 0.05 V s^{-1}(—) and 260 K, 0.4 V s^{-1}(- -), (c) duroquinone; 226 K, 0.05 V s^{-1}(—) and 260 K, 0.2 V s^{-1}(- -) and (d) 2-methyl-1,4-naphthoquinone; 228 K, 0.05 V s^{-1}(—) and 270 K, 0.2 V s^{-1}(- -) in butyronitrile containing 0.06 M of TBAP. The arrows indicate the signal due to the chemical reaction products. The current intensities were normalized for comparison.

$a^{H}_2 = a^{H}_3 = 0.335$ mT, $a^{H}_5 = a^{H}_8 = 0.070$ mT, $a^{H}_6 = a^{H}_7 = 0.150$ mT)[17] were superimposed on the signals of $DQ^{\bullet-}$. To elucidate the phase of the RPM component in $DQ^{\bullet-}$, the contribution of the signals of $DMN^{\bullet+}$ was subtracted using the polynomial function fitting to the broad baselines. The photoinduced ET reaction predominantly proceeds from DMN to excited triplet DQ under the 2.0×10^{-2} M donor concentration, since the lifetime of the excited singlet state of DQ is very short (<5.7 ps).[18] The CIDEP spectra in $DQ^{\bullet-}$ are interpreted by the superposition of the net emission (E) due to the triplet mechanism (TM)[11] and the polarization due to the RPM. The emission signal intensity (indicate by arrow) of $DQ^{\bullet-}$ in the lower magnetic field is weaker than the higher field at 260 K. The phase of the multiplet effect of the RPM is determined to be the absorption/emission (A/E)-type,[9,10] showing the positive J at 260 K. On the contrary, at 213 K, the signal intensity in the lower magnetic field is stronger than that in the higher field. The phase of the RPM is inverted to the E/A-type indicating the negative J. At 226 K, the polarization due to the RPM was hardly observed, representing the negligibly small magnitude of J ($J \sim 0$) at the region of r effective for the RPM generation.[5]

Figure 1b shows the temperature effects on the CIDEP spectra observed in the TMB−MNQ system in BuN. The sharp signals were assigned to the MNQ anion radical ($MNQ^{\bullet-}$) from the g value and HFCs ($g = 2.00429$, $a^{H}_{Me} = 0.298$ mT, $a^{H}_3 = 0.243$ mT, $a^{H}_5 = a^{H}_8 = 0.054$ mT, $a^{H}_6 = a^{H}_7 = 0.071$ mT).[19] The broad emissions superimposed on the signals of $MNQ^{\bullet-}$ were assigned to the TMB cation radical ($TMB^{\bullet+}$) from the reported g value and HFCs of methoxybenzenes.[19] The triplet precursor reaction is also validated because of the fast intersystem crossing from the S_1 state to the T_1 state.[20] As was observed in the DMN-DQ system, the phase of the RPM indicates that the sign of J is inverted from positive to negative with decreasing temperature.

The oxidation ($E^{ox}_{1/2}$) and reduction ($E^{red}_{1/2}$) potentials of the D and A were determined by the CV measurements. Figure 2 shows the temperature dependences of the cyclic voltammograms of (a) DMN, (b) TMB, (c) DQ, and (d) MNQ observed in BuN. The potentials of the $E^{red}_{1/2}$ for the quinones and the $E^{ox}_{1/2}$ values for DMN were determined from the midpoint between the cathodic and anodic peak potentials.[21] In the cyclic voltammograms of TMB, irreversible oxidation waves were observed. The reduction peaks indicated by arrows in (b) are due to the chemical reaction products by the oxidation of TMB.[22] The $E^{ox}_{1/2}$ values for TMB were determined by analyzing the cyclic voltammograms at various sweep rates[23] on the basis of the theory of the stationary electrode polarography[24] (see Supporting Information accompanying this paper). The $-\Delta G_{CR}$ values were obtained from the $E^{ox}_{1/2}$ and $E^{red}_{1/2}$ values by the following equation:[2]

$$-\Delta G_{CR} = E^{ox}_{1/2} - E^{red}_{1/2} \tag{4}$$

The Coulomb attraction term is negligible for the SSRIPs in polar solvents.[25] The $-\Delta G_{CR}$ values were decreased with temperature (Table 1). The temperature dependences of the $-\Delta G_{CR}$ have been interpreted by the entropy changes associated with redox reaction.[26] To clarify the solvent effects on the λ value, we also measured the temperature dependence of the CIDEP spectra for the DMN−DQ system in DMF. The solvent effect on the $-\Delta G_{CR}$ was explained by the difference of the dielectric constants between BuN and DMF.[5] Table 1 summarizes the temperature dependence of the signs of the J and $-\Delta G_{CR}$ observed in the several RIP systems.

Theoretical Analysis of J_{CT} and RPM Polarization. The J of RIP is dominated by the electronic coupling perturbation from the charge-recombined ground state in the triplet reaction precursor system.[13,14] To investigate the inversion of the sign of J depending on temperature or $-\Delta G_{CR}$, theoretical analysis for the J_{CT} has been performed. In the analysis, λ_S is treated by eq 3. In λ_V, the high-frequency intramolecular vibrational modes were taken into account as the accepting modes for the ET reaction. The Franck−Condon (FC) factor for the intramolecular vibrational mode b is expressed with the quantum number j,

$$\mathrm{FC}(j_b) = \exp(-S_b)\frac{S_b^{j_b}}{j_b!} \tag{5}$$

The J_{CT} observed by the RPM CIDEP measurements is the average of the perturbations from all provable solvents and nuclear configurations. The resultant formula for J_{CT} was derived with perturbation theory and was represented as follows:[13]

$$J_{CT}(r) = V(r)^2 \sum_{j_A j_D} \mathrm{FC}(j_A)\mathrm{FC}(j_D) \times \sqrt{\frac{\lambda_S(r)}{2\pi k_B T}} \int_{-\infty}^{\infty} \frac{\exp\left\{-\dfrac{\lambda_S(r)X^2}{2k_B T}\right\} \mathrm{d}X}{\lambda_S(r)(2X-1) - j_D h\nu_D - j_A h\nu_A - \Delta G_{CR}} \tag{6}$$

$$S_D = \frac{\lambda_V^D}{h\nu_D};\ S_A = \frac{\lambda_V^A}{h\nu_A} \tag{7}$$

where X is the normalized solvation coordinate, and $h\nu_D$ and $h\nu_A$ are the local single frequency accepting modes associated with the reorganization of D and A. The term $V(r)$ is dependent upon the distance r as[2,27]

$$V(r) = V_0 \exp\left\{-\frac{\beta}{2}(r-d)\right\} \tag{8}$$

TABLE 1: Temperature Dependence of Signs of J and Driving Forces ($-\Delta G_{CR}$) for Charge Recombination Observed in Several Donor−Acceptor Systems

system							
donor	acceptor	solvent	T/K	sign of J	$E^{ox}_{1/2}$/V[a]	$E^{red}_{1/2}$/V[a]	$-\Delta G_{CR}$ /eV[b]
DMN	DQ	BuN	260	positive	+1.09	−0.84	1.93
			226	$J \sim 0$	+1.06	−0.81	1.87
			213	negative	+1.05	−0.80	1.85
DMN	DQ	DMF	265	positive	+1.11	−0.72	1.83
			240	$J \sim 0$	+1.08	−0.69	1.77
			229	negative	[c]	[c]	[c]
TMB	MNQ	BuN	270	positive	+1.12	−0.78	1.90
			228	$J \sim 0$	+1.07	−0.75	1.82
			215	negative	[c]	[c]	[c]

[a] Obtained by the CV measurements with SCE. [b] Calculated from eq 4. [c] Not measured.

V_0 denotes the electronic coupling matrix element at the closest distance of d.

The $-\Delta G_{CR}$ and r dependences of J_{CT} were simulated by eq 6.[13] The solute and solvent parameters used are listed in Table 2. The solute parameters of d_D and d_A were obtained from the density functional theory (DFT) with GAUSSIAN 98 suite of program.[28] Molecular volumes of the solutes were calculated by the B3LYP density functional with the standard 6-31G* basis set (B3LYP/6-31G* Volume). The d_D and d_A values were determined under the assumption that the solute molecules are spheres. The solvent parameters of n_D and ϵ were utilized from the literature.[29] Although the dielectric parameters vary with temperature, temperature dependence of the λ_S is estimated to be quite small (∼0.01 eV) from eq 3, even when the n_D and ϵ values are utilized under the lower temperature conditions.[30] In the intramolecular vibrational reorganizations, $h\nu_A = h\nu_D = 1500\ cm^{-1}$ corresponding to C═O and C−O stretching modes were considered. The λ_V values were calculated by the DFT method (UB3LYP/6-31G*).[32] The geometries of the radical ions and the neutral ground states were optimized by the DFT method. At the optimized geometries for the ion radicals, the energies in the neutral states were obtained by the single-point calculations. The λ_V values were determined from the energy differences between the two different geometries obtained in the neutral states. The electronic coupling parameters of $V_0 = 300\ cm^{-1}$, $\beta = 11\ nm^{-1}$, and $d = 0.6$ nm were used. These values were obtained from the analysis of the ET reaction rates.[27]

Figure 3a shows the $-\Delta G_{CR}$ dependences of the sign of the J_{CT} calculated by eq 6 at several D−A separations of r (= 1.0, 1.2, 1.5 nm) with the parameters for the DMN-DQ in BuN (system **1**, see Table 2).[33] With the increase in r, the boundary $-\Delta G_{CR}$ value between the positive and negative J_{CT} is increased. Figure 3b shows the $\lambda(r)$ obtained from eqs 2 and 3 for system **1**. From the comparison between Figures 3a and 3b, it is evident, as indicated by the arrows, that the $-\Delta G_{CR}$ value that satisfies $J_{CT} = 0$ well agrees with the total reorganization energy λ at each D−A separation. This result is well consistent with the previous prediction in the triplet-precursor reaction systems;[13,14] when $-\Delta G_{CR}$ is larger than λ, J_{CT} is positive, while in the case of $-\Delta G_{CR} < \lambda$, J_{CT} is negative.

To investigate the RPM CIDEP generated in the RIP systems quantitatively, the RPM electron spin polarization (P_{RPM}) was numerically analyzed by the stochastic Liouville equation (SLE)[34] with taking into account the J_{CT} obtained by eq 6 with the procedures reported in the previous study.[13] In the SLE analysis, molecular diffusion with the mutual diffusion coefficient of D_m, the S−T_0 mixing rate (Q), and the r dependent CR reaction from the singlet RIP were included. The P_{RPM} values were calculated under the condition of $Q = 0.2$ mT. The details of the SLE analysis are described in the Appendix.

Figure 4 shows the $-\Delta G_{CR}$ dependence of the P_{RPM} obtained by the SLE calculation for system **1** using the parameters listed in Table 2. The diffusion coefficients of the D_m in Table 2 were calculated by eqs A14 and A15 under the temperature conditions of $J \sim 0$ obtained. The P_{RPM} values are represented in the units of the thermal equilibrium electron spin polarization P_{eq} ($P_{eq} = 7.4 \times 10^{-4}$) at room temperature. Negative P_{RPM} denotes the E/A type RPM polarization, while the positive P_{RPM} denotes the A/E type polarization. The phase of the RPM is inverted from A/E to E/A with decreasing the $-\Delta G_{CR}$ at the boundary of $-\Delta G_{CR} = 1.76$ eV, which is well consistent with the λ value at the $r = 1.2$ nm separation. The simulated results of Figures 3 and 4 indicate that the P_{RPM} phase reflects the sign of the J_{CT} at the ∼1.2 nm separated RIP systems; $r_{RPM} = 1.2$ nm. Therefore, when the λ is identical with the $-\Delta G_{CR}$ at the 1.2 nm separation, the RPM CIDEP is not generated because of the $J_{CT} = 0$ in the 1.2 nm separated RIP systems. It is concluded, from the model calculations, that the λ value is determined for the 1.2 nm separated D−A system from the $-\Delta G_{CR}$ value for the boundary of RPM phase.[35]

Figure 5a shows the $-\Delta G_{CR}$ dependences of the P_{RPM} calculated with the parameters of systems **2**−**5**. The parameters of the T and D_m were used under the temperature condition of the J∼0 in the TREPR measurements. The boundary values of the $-\Delta G_{CR}$ obtained by the SLE analysis were compared with the total reorganization energy ($\lambda^{calc}_{1.2nm}$) calculated by eqs 2 and 3 with $r = 1.2$ nm in the several D−A systems, as shown in Figure 5b. The boundary values of $-\Delta G_{CR}$ are consistent with the total reorganization energies at the 1.2 nm separations within the deviation < ±0.02 eV. The small deviations of the $\lambda^{calc}_{1.2nm}$ are due to the D_m dependence of the r_{RPM}. We calculated the D_m dependence of the boundary driving force by the SLE analysis, resulting in that the r_{RPM} is decreased with increasing the D_m. This result is explained by the higher reencounter probability at the shorter separation of r with increase in the D_m value. However, the variation of the r_{RPM} is estimated to be smaller than ±0.05 nm under the present experimental study. The results of the SLE analysis clearly demonstrate that individual λ values are experimentally determined at the flexibly separated distance of $r = 1.2$ nm by the observation of the $J \sim 0$ condition.[35]

Discussion

From the SLE analysis, it is obvious that the variations in the $-\Delta G_{CR}$ induce the inversion of the phase of the RPM depending on temperature. The experimental λ values for the several D−A systems were determined for the 1.2 nm separated radical ion pairs from the $-\Delta G_{CR}$ values under the condition that the RPM CIDEP were hardly observed. The uncertainty of the experimental λ value determination comes from the error (<0.01 eV) in the determination of the $-\Delta G_{CR}$ value by the CV measurements. Table 3 summarizes the experimental λ_S values obtained from the λ, λ^D_V and λ^A_V values[36,37] by eq 2 and calculated values (λ^{calc}_S) by eq 3 for the several D−A systems at $r = 1.2$ nm. The experimental λ_S values ranging from 1.27 to 1.39 eV obtained in the present systems agree with the λ^{calc}_S values within the deviation smaller than 0.15 eV. These results show that the Marcus continuum dielectric model well predicts the magnitude of the λ_S for each individual solvent−solute molecular system.

The solvent effect on the λ_S was observed for the DMN−DQ system; $\lambda_S = 1.39$ eV in BuN and $\lambda_S = 1.29$ eV in DMF,

TABLE 2: Parameters Used for the Calculation; Radii (d_D, d_A) and Intramolecular Vibrational Reorganization Energies (λ_V^D, λ_V^A) of Donors and Acceptors, Refractive Indexes (n_D) and Dielectric Constants (ϵ) of Solvents, Temperature and Mutual Diffusion Coefficients (D_m)

		solute parameter				solvent parameter			
no.	system	d_D/nm[a]	d_A/nm[a]	λ_V^D/eV[b]	λ_V^A/eV[b]	n_D[c]	ϵ[c]	T/K[d]	D_m/m^2 s^{-1}[e]
1	DMN-DQ in BuN	0.390	0.358	0.23	0.25	1.38	20.3	226	4.9×10^{-10}
2	DMN-DQ in DMF	0.390	0.358	0.23	0.25	1.43	36.7	240	4.7×10^{-10}
3	TMB-MNQ in BuN	0.369	0.374	0.31	0.22	1.38	20.3	228	5.2×10^{-10}
4	TMB-DQ in BuN	0.369	0.358	0.31	0.25	1.38	20.3	249	8.7×10^{-10}
5	TMB-DQ in DMF	0.369	0.358	0.31	0.25	1.43	36.7	258	6.9×10^{-10}

[a] Calculated from the DFT method (B3LYP/6-31G* Volume). [b] Determined from the DFT method (UB3LYP/6-31G*). [c] From ref 29. [d] Temperature under the $J \sim 0$ condition. [e] Calculated from eqs A14 and A15 at the temperature under the $J \sim 0$ condition.

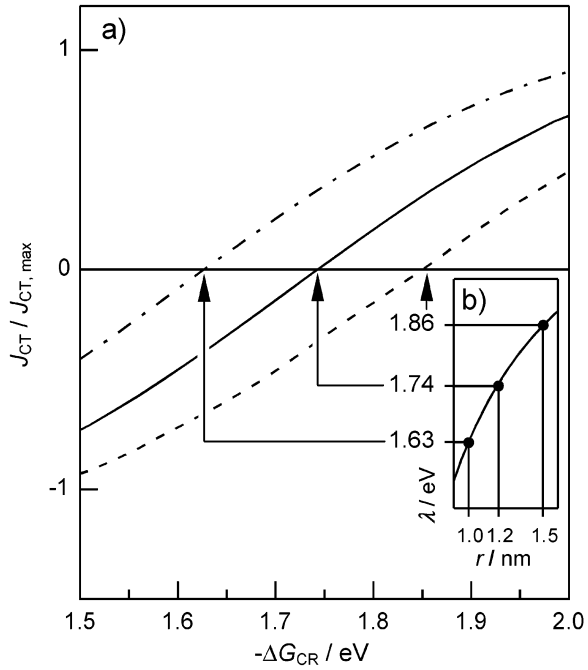

Figure 3. (a) Driving force ($-\Delta G_{CR}$) dependences of the singlet−triplet energy splitting (J_{CT}) obtained by eq 6 with the parameters of the 1,4-dimethoxynaphthalene-duroquinone system in butyronitrile (system **1**) at the donor−acceptor separation of the $r = 1.0$ nm (- · -), $r = 1.2$ nm (—), and $r = 1.5$ nm (- -). (b) The r dependence of the total reorganization energy (λ) calculated from eqs 2 and 3 with the parameters of system **1**.

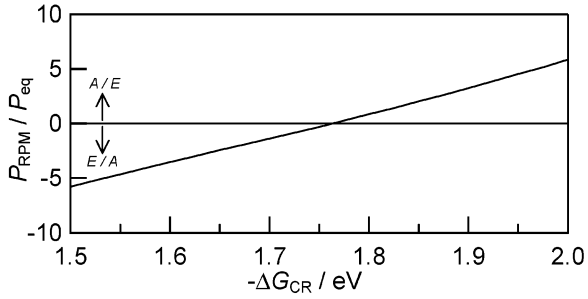

Figure 4. Driving force ($-\Delta G_{CR}$) dependence of the RPM polarization (P_{RPM}) calculated from the SLE analysis with the parameters of the 1,4-dimethoxynaphthalene-duroquinone system in butyronitrile (system **1**).

respectively. This fact agrees with that observed in the TMB−DQ system.[5] The effect is well explained by the difference of the solvent parameters (n_D and ϵ) between BuN and DMF.

When the λ_S values determined for the TMB−MNQ (system **3**) and TMB−DQ (system **4**) systems in BuN are compared, the value of the former system is smaller than that of the latter. This is interpreted in terms of the molecular size effect because

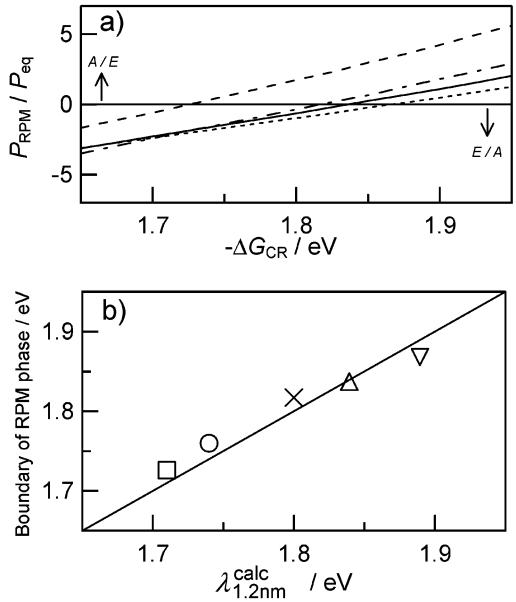

Figure 5. (a) Driving force ($-\Delta G_{CR}$) dependences of magnitude of the RPM polarization (P_{RPM}) calculated from the SLE analysis with the parameters of system **2** (- - -), system **3** (- · - ·), system **4** (·····), and system **5** (—). (b) Plots of driving force for the boundary of RPM phase versus total reorganization energy ($\lambda_{1.2nm}^{calc}$) calculated by eqs 2 and 3 with the donor−acceptor distance of $r = 1.2$ nm; system **1** (○), system **2** (□), system **3** (×), system **4** (▽), and system **5** (△). The driving force for the boundary was obtained from the SLE analysis in each D−A system.

TABLE 3: Reorganization Energies (λ) and Solvent Reorganization Energies (λ_S) Determined by TREPR Measurements and λ and λ_S Values Calculated by Eqs 2 and 3 with the Donor−Acceptor Distance of $r = 1.2$ nm

	TREPR measurements		continuum dielectric model	
no.	λ ($\pm$0.02) /eV[a]	λ_S ($\pm$0.02)/eV[b]	$\lambda_{1.2nm}^{calc}$/eV[c]	λ_S^{calc}/eV[d]
1	1.87	1.39	1.74	1.26
2	1.77	1.29	1.71	1.23
3	1.82	1.29	1.80	1.27
4	1.92[e]	1.36[e]	1.89	1.33
5	1.83[e]	1.27[e]	1.84	1.28

[a] Determined from $\lambda = -\Delta G_{CR} = E_{1/2}^{ox} - E_{1/2}^{red}$ under the conditions of $J \sim 0$. [b] Obtained from eq 2. [c] Calculated from eq 2. [d] Calculated from eq 3 with $r = 1.2$ nm. [e] From ref 5.

the calculations well reproduce the difference of the λ_S values as shown in Table 3. The experimental λ_S values agree quantitatively with the calculated values in systems **3**, **4**, and **5**. In contrast, the experimental λ_S values in systems **1** and **2**, which involve DMN as the electron donor, are larger by ~0.1 eV than the λ_S^{calc} values. It has been suggested that the steric hindrance of the solute molecules may affect the effective separation of r for the ET reactions.[8] The interaction between the solute

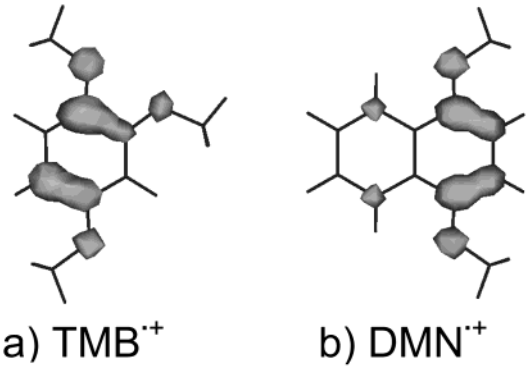

Figure 6. Spin density distribution for the cation radicals of (a) 1,2,4-trimethoxybenzene ($TMB^{\bullet+}$) and (b) 1,4-dimethoxynaphthalene ($DMN^{\bullet+}$) calculated by the density functional theory (UB3LYP/6-31G*).

molecules is, however, negligible in the present TREPR experiments because of the long distance between the pair radical ions of 1.2 nm. According to the solvent-mediated electronic coupling mechanism,[38] V or β in eq 8 is dependent on $-\Delta G_{CR}$. This effect might make the effective separation of the r_{RPM} larger in the DMN−DQ system than in the TMB−DQ system. However, this contribution is also excluded, since the $-\Delta G_{CR}$ is smaller in the DMN−DQ system than that in the TMB−DQ system. Details are described in Supporting Information.

Kitamura et al. estimated the λ_S values in photoredox quenching of a ruthenium(II) complex by aromatic amines.[39] The estimated λ_S values were larger than those calculated from eq 3. They suggested that solvent reorganization around the amino group is more relevant than that around a whole molecule, since the orbital involved in the ET process is localized on the nitrogen atom of amines. In methoxy-substituted aromatic hydrocarbons, the spin density on the cation radicals tends to localize around the methoxy substitutions.[40] Figure 6 shows the spin density distributions in the cation radicals of $TMB^{\bullet+}$ and $DMN^{\bullet+}$ calculated by the DFT method (UB3LYP/6-31G*). In $TMB^{\bullet+}$ and $DMN^{\bullet+}$, the spin densities are concentrated around the methoxy substitutions, reflecting single occupied molecular orbital of cations. In $TMB^{\bullet+}$, the spin density is distributed on the whole molecule, because the three methoxy substitutions attach to one benzene ring. On the other hand, in $DMN^{\bullet+}$, more than 80% of spin density is distributed on the methoxy-substituted benzene ring moiety. The effective orbital size for the solvent reorganization should be smaller than the estimated molecular size of DMN, because the orbital involved in the ET reaction is more localized than the total electron density.[40,41] Thus, the determined λ_S values in the DMN−DQ systems are larger than that calculated by eq 3 with the d_D obtained from the molecular volume calculation of DMN.

Conclusion

The individual λ and λ_S values were determined for the CR process involving the quinone anion radicals and methoxy-substituted aromatic cation radicals in BuN and DMF from the observation of the RPM CIDEP generated through the photo-induced intermolecular ET reaction. By probing the singlet−triplet energy gap of the J created in the RIPs, the λ and λ_S values were simply determined from the $-\Delta G_{CR}$ values under the $J\sim0$ conditions. The determined λ_S values were consistent with those calculated from eq 3 with the deviation of ~0.1 eV. The experimental results indicate that the Marcus continuum dielectric model is well applicable for the flexible 1.2 nm separated RIP systems in the polar solvents, when the appropriate molecular sizes are chosen to evaluate the λ_S values. Especially, it is found that the spin density localization of the ion radical leads to larger λ_S values than those predicted with the molecular sizes from the total electron density obtained by the molecular volume calculations.

Appendix

The SLE, including the effects of spin interaction, molecular diffusion, and CR reaction (k_{CR}) is written as follows:[34]

$$\frac{\partial r\rho(r,t)}{\partial t} = -i[\boldsymbol{H}_{RIP}(r),\, r\rho(r,t)] + D_m\frac{\partial^2 r\rho(r,t)}{\partial r^2} + \boldsymbol{K}(r)r\rho(r,t) \tag{A1}$$

where $\rho(r,t)$ is the density matrix of the RIP at time t and r. $\boldsymbol{K}(r)$ is the superoperator for the CR reactions. The spin Hamiltonian is composed of the Zeeman effect, hyperfine interaction, and $J(r)$ and is represented as follows:

$$\boldsymbol{H}_{RIP}(r) = \beta_e\hbar(g_aS_{az} + g_cS_{cz})\boldsymbol{B}_0 - J(r)\left(2\boldsymbol{S}_a\boldsymbol{S}_c + \frac{1}{2}\right) + \sum_l A_{al}\boldsymbol{I}_{al}\boldsymbol{S}_a + \sum_n A_{cn}\boldsymbol{I}_{cn}\boldsymbol{S}_c \tag{A2}$$

The subscripts a and c represent the anion and cation radicals that form the RIP. A is the hyperfine coupling constant of atom l in anion radicals and atom n in cation radicals. The matrix elements of the $H_{RIP}(r)$ in the $S-T_0$ system are represented with high magnetic field approximation as follows:

$$\begin{matrix} & |S\rangle & |T_0\rangle \end{matrix}$$

$$\boldsymbol{H}_{RIP}(r) = \begin{bmatrix} 2J(r) & Q \\ Q & 2J(r) \end{bmatrix} \tag{A3}$$

The J of RIP is treated with eq 4 and assumed as $2J(r) = J_{CT}(r)$. The off-diagonal part of the Q is written as

$$Q = \frac{1}{2}(g_a - g_c)\beta_e\hbar B_0 + \frac{1}{2}\left(\sum_l A_{al}m_{al} - \sum_n A_{cn}m_{cn}\right) \tag{A4}$$

The $2Q$ term is the difference of EPR resonant frequencies between the anion and cation radicals and determines the $S-T_0$ mixing rate. The matrix elements $[\boldsymbol{H}_{RIP}(r),\, \rho\,(r,t)]$, obtained from eqs. A2−A4, are described as follows:

$$[\boldsymbol{H}_{RIP}(r),\rho(r,t)] = \begin{bmatrix} 0 & -Q & Q & 0 \\ -Q & 2J(r) & 0 & Q \\ Q & 0 & -2J(r) & -Q \\ 0 & Q & -Q & 0 \end{bmatrix}\begin{bmatrix} \rho_{SS} \\ \rho_{ST_0} \\ \rho_{T_0S} \\ \rho_{T_0T_0} \end{bmatrix} \tag{A5}$$

Here, ρ represents the matrix element of the density matrix, $\rho_{SS} = C_SC_S^*$, $\rho_{ST_0} = C_SC_{T_0}^*$, $\rho_{T_0S} = C_{T_0}C_S^*$, and $\rho_{T_0T_0} = C_{T_0}C_{T_0}^*$, where $C_S(r,t)$ and $C_{T_0}(r,t)$ are the coefficients of the wave function, $\psi(r,\, t) = C_S(r,\, t)|S\rangle + C_{T_0}(r,t))|T_0\rangle$, in the SLE. The CR reaction operator of $\boldsymbol{K}(r)$ is described as

$$\boldsymbol{K}(r)\rho(r,t) = -\frac{k_{CR}(r)}{2}\{|S\rangle\langle S|\rho(r,t) + \rho(r,t)|S\rangle\langle S|\} \tag{A6}$$

The CR reactions proceed from the singlet RIP. The term $k_{CR}(r)$ is the probability of the CR reaction and represented as[42]

$$k_{CR}(r) = \sqrt{\frac{\pi}{\hbar^2 \lambda_S(r) k_B T}} V(r)^2 \sum_{j_A, j_D} FC(j_A) FC(j_D) \times \exp\left[-\left\{ \frac{\lambda_S(r) + \Delta G_{CR} + j_D h\nu_D + j_A h\nu_A}{4\lambda_S(r) k_B T} \right\} \right] \quad \text{(A7)}$$

The diffusion of the ion radicals in the RIP was assumed as the simple Brownian motion[43] and treated by the finite difference technique with the mutual diffusion coefficient of D_m as follows:

$$D_m \frac{\partial^2 \hat{\rho}(r,s)}{\partial r^2} = D_m \frac{\hat{\rho}(r - \Delta r_k, s) - 2\hat{\rho}(r_k, s) + \hat{\rho}(r + \Delta r_k, s)}{\Delta r_k^{\,2}} \quad \text{(A8)}$$

$$\hat{\rho}(r,t) = r\rho(r,t) \quad \text{(A9)}$$

where Δr_k is small but finite increment in r. The application of the finite difference technique is essentially equivalent to transforming the continuous diffusion equation into a discrete master equation involving a transition probability matrix $\boldsymbol{W}$. The $\boldsymbol{W}$ couples $\hat{\rho}(r,t)$ between discrete values $\hat{\rho}(d + u\Delta r, t)$, where $u = 0,1,2,....$, in the case that one Δr value is used for the calculation. These discrete values form a column vector $\hat{\rho}(r,t)$.

$$D_m \frac{\partial^2 r\rho(r,t)}{\partial r^2} \rightarrow \boldsymbol{W}\hat{\rho}(r,t) \quad \text{(A10)}$$

In the analysis, we set 40 segments in the distance r from the closest distance of the d. The Δr_k values were $\Delta r_1 = 0.025$ nm in the first 10 segments, $\Delta r_2 = 0.05$ nm in the second 10 segments, $\Delta r_3 = 0.1$ nm in the third 10 segments, and $\Delta r_4 = 1$ nm in the last 10 segments. The total transition-probability matrix element of $\boldsymbol{W}$ is given as

$$\boldsymbol{W} = D_m \begin{array}{c} \begin{array}{cccccccccccc} 1 & & 2 & 3 & 4 & \cdots & u & \cdots & 37 & 38 & 39 & 40 \end{array} \\ \begin{pmatrix} \frac{-2[1+(\Delta r_1/d)]}{\Delta r_1^{\,2}} & \frac{2}{\Delta r_1^{\,2}} & & & & & & & & & & \\ \frac{1}{\Delta r_1^{\,2}} & \frac{-2}{\Delta r_1^{\,2}} & \frac{1}{\Delta r_1^{\,2}} & & & & & & & & & \\ & \frac{1}{\Delta r_1^{\,2}} & \frac{-2}{\Delta r_1^{\,2}} & \frac{1}{\Delta r_1^{\,2}} & & & & & & & & \\ & & \cdot & \cdot & \cdot & & & & & & & \\ & & & \cdot & \cdot & \cdot & & & & & & \\ & & & & \cdot & \cdot & \cdot & & & & & \\ & & & & & \cdot & \cdot & \cdot & & & & \\ & & & & & & & \frac{1}{\Delta r_4^{\,2}} & \frac{-2}{\Delta r_4^{\,2}} & \frac{1}{\Delta r_4^{\,2}} & & \\ & & & & & & & & \frac{1}{\Delta r_4^{\,2}} & \frac{-2}{\Delta r_4^{\,2}} & 0 & \\ & & & & & & & & & \frac{2}{\Delta r_4^{\,2}} & 0 & \end{pmatrix} \end{array} \quad \text{(A11)}$$

where the first row represents the condition of the reflecting wall at d. The last row represents that the RIPs collect at the last segment ($r > 11.325$ nm), and cannot diffuse back. In the matrix $\boldsymbol{W}$, the Δr changes from Δr_k to Δr_{k+1}, at the 10th, 20th, and 30th rows. In these rows, the elements of the $\boldsymbol{W}$ are given by

$$W_{u,u-1} = \left(\frac{2}{1+f}\right)\left(\frac{D_m}{\Delta r_k}\right)$$

$$W_{u,u} = -\left(\frac{2}{f}\right)\left(\frac{D_m}{\Delta r_k}\right) \quad \text{(A12)}$$

$$W_{u,u+1} = \left[\frac{2}{(1+f)f}\right]\left(\frac{D_m}{\Delta r_k}\right)$$

$$f = \frac{\Delta r_{k+1}}{\Delta r_k} \quad \text{(A13)}$$

D_m is the sum of the diffusion coefficient of the anion and cation radicals; $D_m = D_a + D_c$. The diffusion coefficient (D_S) for the solute is represented as the Stokes−Einstein equation with the solvent viscosity (η) and radius (d_S) of solute,[44,45]

$$D_S(T) = \frac{k_B T}{6\pi\eta d_S} \quad \text{(A14)}$$

The radii of the cation and anion radicals were utilized from the results of the DFT calculations. The temperature dependence of the η is approximately expressed as the Arrhenius form with the preexponential factor (C) and activation energy (E_a),[46]

$$\eta(T) = C \times \exp\left(\frac{E_a}{RT}\right) \quad \text{(A15)}$$

where R is the gas constant. The C and E_a for BuN and for DMF were estimated from the literature. The estimated values were $C = 1.29 \times 10^{-5}$ Pa s and $E_a = 9.29 \times 10^3$ J mol^{-1} for BuN and $C = 2.76 \times 10^{-5}$ Pa s and $E_a = 8.56 \times 10^3$ J mol^{-1} for DMF, respectively.[29]

The Laplace formation of the eq A1 results is

$$s\hat{\rho}(r,s) - r\rho_0(r,t=0) = -i[\boldsymbol{H}_{RIP}(r), \hat{\rho}(r,s)] + D_m \frac{\partial^2 \hat{\rho}(r,s)}{\partial r^2} + \boldsymbol{K}(r)\hat{\rho}(r,s) \quad \text{(A16)}$$

where

$$\hat{\rho}(r,s) = \int_0^\infty e^{-st} \hat{\rho}(r,t)\, dt \quad \text{(A17)}$$

The RPM polarization in the anion radical is given by

$$P_{RPM} = -2\lim_{s\to 0} s \int_d^\infty tr\{r\hat{\rho}(r,s) S_{az}\}\, dr \quad \text{(A18)}$$

In the SLE analysis, we assumed that the RIPs were initially populated by three-triplet states (T_0, T_+, T_-) equally at the closest distance d. This assumption has been ascertained for the photoinduced charge separation (CS) reaction systems in which the RIPs generated via the exciplexes, when the driving force ($-\Delta G_{CS}$) for CS is smaller than ~1 eV.[6d]

Supporting Information Available: Additional experimental details. This material is available free of charge via the Internet at http://pubs.acs.org.

References and Notes

(1) Masuhara, H.; Mataga, N. *Acc. Chem. Res.* **1981**, *14*, 312.
(2) (a) Kavarnos, G. J.; Turro, N. J. *Chem. Rev.* **1986**, *86*, 401. (b) Marcus, R. A.; Sutin, N. *Biochim. Biophys. Acta* **1985**, *811*, 265.

(3) (a) Marcus, R. A. *J. Chem. Phys*. **1956**, *24*, 966. (b) Marcus, R. A. *J. Chem. Phys*. **1956**, *24*, 979.

(4) Mataga, N.; Asahi, T.; Kanda, Y.; Okada, T. *Chem. Phys*. **1988**, *127*, 249.

(5) Kobori, Y.; Yago, T.; Akiyama, K.; Tero-Kubota, S. *J. Am. Chem. Soc*. **2001**, *123*, 9722.

(6) (a) Gould, I. R.; Ege, D.; Moser, J. E.; Farid, S. *J. Am. Chem. Soc*. **1990**, *112*, 4290. (b) Gould, I. R.; Young, R. H.; Moody, R. E.; Farid, S. *J. Phys. Chem*. **1991**, *95*, 2068. (c) Gould, I. R.; Farid, S. *Acc. Chem. Res*. **1996**, *29*, 522. (d) Kikuchi, K.; Niwa, T.; Takahashi, Y.; Ikeda, H.; Miyashi, T. *J. Phys. Chem*. **1993**, *97*, 5070.

(7) Tachiya, M.; Murata, S. *J. Phys. Chem*. **1992**, *96*, 8441.

(8) (a) Gould, I. R.; Farid, S. *J. Phys. Chem*. **1993**, *97*, 13067. (b) Vauthey, E. *J. Phys. Chem. A* **2000**, *104*, 1804.

(9) Muss, L. T.; Atkins, P. W.; McLauchlan, K. A.; Pedersen, J. B. *Chemically induced magnetic polarization*; Reidel: Dordrecht, 1977.

(10) (a) Doktorov, A. B.; Neufeld, A. A.; Pedersen, J. B. *J. Chem. Phys*. **1999**, *110*, 8881. (b) Adrian, F. J. *J. Chem. Phys*. **1971**, *54*, 3918. (c) Monchick, L.; Adrian, F. J. *J. Chem. Phys*. **1978,** *68*, 4376.

(11) (a) Atkins, P. W.; Evans, G. T.; *Mol. Phys*. **1975**, *29*, 921. (b) Pedersen, J. B.; Freed, J. H. *J. Chem. Phys*. **1975**, *62*, 1706.

(12) (a) Tachikawa, T.; Kobori, Y.; Akiyama, K.; Katsuki, A.; Usui, Y.; Steiner, U.; Tero-Kubota, S.; *Mol. Phys*. **2002**, *100*, 1413. (b) Tero-Kubota, S.; Katsuki, A.; Kobori, Y. *J. Photochem. Photobiol. C* **2001**, *2*, 17.

(13) Kobori, Y.; Akiyama, K.; Tero-Kubota, S. *J. Chem. Phys*. **2000**, *113*, 465.

(14) (a) Kobori, Y.; Sekiguchi, S.; Akiyama, K.; Tero-Kubota, S. *J. Phys. Chem. A* **1999**, *103*, 5416. (b) Sekiguchi, S.; Kobori, Y.; Akiyama, K.; Tero-Kubota, S. *J. Am. Chem. Soc*. **1998**, *120*, 1325.

(15) (a) Volk, M.; Häberle, T.; Feick, R.; Ogrodnik, A.; Michel-Beyerle, M. E. *J. Phys. Chem*. **1993**, *97*, 9831. (b) Bixon, M.; Jortner, J.; Michel-Beyerle, M. E. *Z. Phys. Chem*. (Munich) **1993**, *180*, 193.

(16) Segal, B. G.; Kaplan, M.; Fraenkel, G. K. *J. Chem. Phys*. **1965**, *43*, 4191.

(17) Sullivan, P. D. *J. Phys. Chem*. **1970**, *74*, 2563.

(18) Nagaoka, S.; Ishihara, K. *J. Am. Chem. Soc*. **1996**, *118*, 7361.

(19) Pedersen, J. A. *Handbook of EPR spectra from quinones and quinols*; CRC: Boca Raton, 1985.

(20) Sakaguchi, Y.; Hayashi, H. *J. Phys. Chem*. **1984**, *88*, 1437.

(21) (a) For the reported $E_{1/2}^{red}$ values of quinones in DMF, see Fritsch, J. M.; Tatwawadi, S. V.; Adams, R. N. *J. Phys. Chem*. **1967**, *71*, 338. (b) For the reported $E_{1/2}^{ox}$ values of DMN in acetonitrile, see: Zweig, A.; Maurer, A. H.; Roberts, B. G. *J. Org. Chem*. **1967**, *32*, 1322.

(22) The electrochemical oxidations of the methoxybenzenes have been known to cause dimerization reactions in methanolic potassium hydroxide solution. Belleau, B.; Weinberg, N. L. *J. Am. Chem. Soc*. **1963**, *85*, 2525.

(23) Fukuzumi, S.; Koumitsu, S.; Hironaka, K.; Tanaka, T. *J. Am. Chem. Soc*. **1987**, *109*, 305.

(24) (a) Nicholson, R. S.; Shain, I. *Anal. Chem*. **1964**, *36*, 706. (b) Klingler, R. J.; Kochi, J. K. *J. Am. Chem. Soc*. **1982**, *104*, 4186.

(25) Knibbe, H.; Rehm, D.; Weller, A. *Ber. Bunsen-Ges. Phys. Chem*. **1968**, *72*, 257. (b) Arnold, B. R.; Farid, S.; Goodman, J. L.; Gould, I. R. *J. Am. Chem. Soc*. **1996**, *118*, 5482.

(26) (a) Nagaoka, T.; Okazaki, S. *J. Phys. Chem*. **1985**, *89*, 2340. (b) Bilio, A. J. D.; Hill, M. G.; Bonander, N.; Karlsson, B. G.; Villahermosa, R. M.; Malmström, B. G.; Winkler, J. R.; Gray, H. B. *J. Am. Chem. Soc*. **1997**, *119*, 9921.

(27) V_0 values are reported to be $V_0 = 300$ cm^{-1} at $d \sim 0.6$ nm separation. β is known to be within the range from 9 ot 12 nm^{-1}; see (a) Tavernier, H. L.; Kalashnikov, M. M.; Fayer, M. D. *J. Chem. Phys*. **2000**, *113*, 10191. (b) Closs, G. L.; Miller, J. R. *Science* **1988**, *240*, 440.

(28) Frisch, M. J.; Trucks, G. W.; Schlegel, H. B.; Scuseria, G. E.; Robb, M. A.; Cheeseman, J. R.; Zakrzewski, V. G.; Montgomery, J. A., Jr.; Stratmann, R. E.; Burant, J. C.; Dapprich, S.; Millam, J. M.; Daniels, A. D.; Kudin, K. N.; Strain, M. C.; Farkas, O.; Tomasi, J.; Barone, V.; Cossi, M.; Cammi, R.; Mennucci, B.; Pomelli, C.; Adamo, C.; Clifford, S.; Ochterski, J.; Petersson, G. A.; Ayala, P. Y.; Cui, Q.; Morokuma, K.; Malick, D. K.; Rabuck, A. D.; Raghavachari, K.; Foresman, J. B.; Cioslowski, J.; Ortiz, J. V.; Baboul, A. G.; Stefanov, B. B.; Liu, G.; Liashenko, A.; Piskorz, P.; Komaromi, I.; Gomperts, R.; Martin, R. L.; Fox, D. J.; Keith, T.; Al-Laham, M. A.; Peng, C. Y.; Nanayakkara, A.; Gonzalez, C.; Challacombe, M.; Gill, P. M. W.; Johnson, B.; Chen, W.; Wong, M. W.; Andres, J. L.; Gonzalez, C.; Head-Gordon, M.; Replogle, E. S.; Pople, J. A. *Gaussian 98*; Gaussian, Inc.: Pittsburgh, PA, 1998.

(29) Riddick J. A.; Bundger, W. B. *Organic solvents*; Wiley & Sons: New York, 1970. Reported values of η were 6.24×10^{-4} Pa s at 288 K for BuN and 9.243×10^{-4} Pa s at 293 K for DMF.

(30) In typical organic solvents, the temperature dependences of n_D and ϵ are $dn_D/dT \sim -4.5 \times 10^{-4}$ K^{-1}, and $(\ln\epsilon)/dT = -3 \times 10^{-1} \sim -7 \times 10^{-1}$ K^{-1} (see ref 31). In BuN and DMF, the temperature dependence of the n_D and ϵ were assumed as follows; $dn_D/dT = -4.5 \times 10^{-4}$ K^{-1}, $d(\ln\epsilon)/dT = -7 \times 10^{-1}$ K^{-1}. The difference in calculated λ_S values is ~0.01 eV in BuN and ~0.02 eV in DMF under the temperature regions in this study.

(31) Marcus, Y. *Introduction to liquid-state chemistry*; Wiley & Sons: New York, 1977.

(32) (a) Nelsen, S. F.; Blackstock, S. C.; Kim, Y. *J. Am. Chem. Soc*. **1987**, *109*, 677. (b) Brouwer, A. M.; *J. Phys. Chem. A* **1997**, *101*, 3626. (c) Balakrishnan, G.; Keszthelyi, T.; Wilbrandt, R.; Zwier, J. M.; Brouwer, A. M.; Buma, W. J. *J. Phys. Chem. A* **2000**, *104*, 1834.

(33) In the J_{CT} calculation, it was confirmed that the boundary $-\Delta G_{CR}$ value between the $J_{CT} < 0$ and $J_{CT} > 0$ did not vary with temperature.

(34) (a) Pedersen, J. B.; Freed, J. H. *J. Chem. Phys*. **1973**, *58*, 2746. (b) Pedersen, J. B.; Freed, J. H. *J. Chem. Phys*. **1973**, *59*, 2869.

(35) In this study, $d = 0.6$ nm was used for the calculation, since we assumed that the solutes are sphere (d_D, $d_A = 0.3 \sim 0.4$ nm). When the disk model is applied to the solute shapes, the D−A distance was estimated to be ~0.35 nm (see ref 6b) in the contact radical ion pair. In the case of $d = 0.35$ nm, the r_{RPM} was also calculated to be $r_{RPM} = 1.2$ nm with the parameters of $V_0 = 600$ cm^{-1} and $\beta = 10$ nm^{-1}, as was described in ref 5. When $\beta = 10$ nm^{-1}, $d = 0.6$ nm, and $V_0 = 300$ cm^{-1} are used for the SLE analysis, $r_{RPM} = 1.3$ nm is obtained. Therefore, it is expected that the error in the effective separation is within 0.1 nm due to the uncertainty of the parameters in the electronic coupling. The deviation of the λ_S value is adequately small (<0.05 eV) between $r = 1.2$ and 1.3 nm in eq 3.

(36) The validity of the UB3LYP/6-31G* level calculation of the λ_V^D value was confirmed by a comparison with intramolecular reorganization energy for ionization of 1,4-diaza[2.2.2]bicyclooctane (DABCO) obtained with the difference between the vertical and adiabatic ionization potentials (see ref 32c).

(37) The λ_V differences between TMB and DMN are interpreted by the variation of the number of the methoxy substitutions. According to ref 40, one of the intramolucular reorganizations with ET is the change of the C−O bond length in the methoxy-substituted aromatic hydrocarbons. It is expected that the increase of the number of the methoxy substitutions results in the increase of the λ_V values. This consideration was confirmed by the DFT calculations. The λ_V^D values for anisol (AN) and 1,4-dimethoxybenzen (DMB) were calculated to be $\lambda_V^{AN} = 0.22$ eV and $\lambda_V^{DMB} = 0.28$ eV by the DFT method. In the DFT calculations, it was also found that the λ_V^D values in methoxynaphthalenes are smaller than those in methoxybenzens, when the number of the methoxy substitution is the same. The spread of π conjugate system may restrict the molecular structure change associated with ET, resulting the reduction of the λ_V^D values in the methoxynaphthalenes.

(38) (a) Newton, M. D. *Chem. Rev*. **1991**, *91*, 767. (b) Paddon-Row, M. N. *Acc. Chem. Res*. **1994**, *27*, 18. (c) McConnell, H. M. *J. Chem. Phys*. **1961**, *35*, 508.

(39) Kitamura, N.; Kim, H. B.; Okano, S.; Tazuke, S. *J. Phys. Chem*. **1989**, *93*, 5750.

(40) Zweig, A.; Hodgson, W. G.; Jura, W. H. *J. Am. Chem. Soc*. **1964**, *86*, 4124.

(41) About 70% of the total spin density is localized on the carbonyl group (C═O) of the MNQ anion radical. Similar spin density localization is also calculated in DQ$^{\bullet-}$. However, these quinone anion radicals do not show significant localization effects on the reorganization energies.

(42) Hopfield, J. J. *Proc. Natl. Acad. Sci. U. S. A*. **1974**, *71*, 3640.

(43) The Coulomb interaction between the pair ion radicals is neglected in the present work, because the interaction is considered to be negligibly small in the nanometer separated RIPs in polar solvents ($\epsilon > 20$).[25] The contact RIP generated by photoinduced electron transfer may rapidly solvate to form a solvent-separated RIP in polar solvents. The RPM CIDEP due to the S−T$_0$ mixing is effectively created where the magnitude of the 2J is comparable to the hyperfine interaction.

(44) Cussler, E. L. *Diffusion, mass transfer in fluid system*; Cambridge University Press: Cambridge, 1997.

(45) Radical diffusion rates have been found to agree well with the Stokes−Einstein equation; see Terazima, M.; Okamoto, K.; Hirota, N. *J. Chem. Phys*. **1995**, *102*, 2506.

(46) Kierstead, H. A.; Turkevich, J. *J. Chem. Phys*. **1944**, *12*, 24.